








Type II Supernova Light Curves and Spectra from the CfA

Malcolm Hicken¹, Andrew S. Friedman^{1,2,3} , Stephane Blondin⁴ , Peter Challis¹, Perry Berlind¹, Mike Calkins¹ , Gil Esquerdo⁵, Thomas Matheson⁶ , Maryam Modjaz⁷ , Armin Rest⁸, and Robert P. Kirshner^{1,9}

¹Harvard-Smithsonian Center for Astrophysics, Cambridge, MA 02138, USA

²Center for Theoretical Physics and Department of Physics, Massachusetts Institute of Technology, Cambridge, MA 02139, USA

³University of California, San Diego, La Jolla, CA 92093, USA

⁴Aix Marseille Univ, CNRS, LAM, Laboratoire d'Astrophysique de Marseille, Marseille, France

⁵Planetary Science Institute, 1700 East Fort Lowell Road, Tucson, AZ 85719, USA

⁶National Optical Astronomy Observatory, 950 North Cherry Avenue, Tucson, AZ, 85719, USA

⁷Center for Cosmology and Particle Physics, New York University, 4 Washington Place, New York, NY 10003, USA

⁸Space Telescope Science Institute, Baltimore, MD 21218, USA

⁹Gordon and Betty Moore Foundation, 1661 Page Mill Road, Palo Alto, CA 94304, USA

Received 2017 June 13; revised 2017 September 6; accepted 2017 September 14; published 2017 November 10

Abstract

We present multiband photometry of 60 spectroscopically confirmed supernovae (SNe): 39 SNe II/IIP, 19 IIn, 1 IIb, and 1 that was originally classified as a IIn but later as a Ibn. Of these, 46 have only optical photometry, 6 have only near-infrared (NIR) photometry, and 8 have both optical and NIR. The median redshift of the sample is 0.016. We also present 195 optical spectra for 48 of the 60 SN. There are 26 optical and 2 NIR light curves of SNe II/IIP with redshifts $z > 0.01$, some of which may give rise to useful distances for cosmological applications. All photometry was obtained between 2000 and 2011 at the Fred Lawrence Whipple Observatory (FLWO), via the 1.2 m and 1.3 m PAIRITEL telescopes for the optical and NIR, respectively. Each SN was observed in a subset of the $u'UBVRi'i'JHK_s$ bands. There are a total of 2932 optical and 816 NIR light curve points. Optical spectra were obtained using the FLWO 1.5 m Tillinghast telescope with the FAST spectrograph and the MMT Telescope with the Blue Channel Spectrograph. Our photometry is in reasonable agreement with select samples from the literature: two-thirds of our star sequences have average V offsets within ± 0.02 mag and roughly three-quarters of our light curves have average differences within ± 0.04 mag. The data from this work and the literature will provide insight into SN II explosions, help with developing methods for photometric SN classification, and contribute to their use as cosmological distance indicators.

Key words: supernovae: general

Supporting material: data behind figure, machine-readable tables

1. Introduction

This paper presents Center for Astrophysics (CfA) SN II light curves and spectra, all of which are publicly available from the journal, the CfA SN Group web site,¹⁰ and The Open Supernova Catalog.¹¹ It is our hope that these data will be of use to the broader SN community for use in SN II analysis and cosmological calculations.

Massive stars ($M \gtrsim 8 M_{\odot}$) end their lives as core-collapse supernovae (CCSNe). Those that have retained a large portion of their hydrogen envelope are known as Type II SNe, with spectra dominated by Balmer features. Those that have lost their hydrogen envelope and have no Balmer lines, but have helium features, are known as Type Ib. Finally, those that have also lost much or all of their helium envelope and show no helium spectral features are known as Type Ic. For reviews of these classifications, see, for example, Gal-Yam (2016) and the introductions of Smartt et al. (2009), Van Dyk et al. (2012), Modjaz et al. (2016), and Liu et al. (2016). A continuum seems to exist across the CCSNe classes, depending on how much of

the outer layer(s) has been lost. SNe II with thick hydrogen envelopes have a long plateau phase with roughly constant or slowly declining luminosity (SNe IIP), whereas those with thinner envelopes decline more quickly (SNe IIL; see, for example: Anderson et al. 2014; Sanders et al. 2015). Gall et al. (2015) point out that, in addition to thinner envelopes, SNe IIL need larger progenitor radii than SNe IIP to give rise to their observed luminosities. There also appears to be a continuous range of decline rates joining SNe IIP and IIL, giving further weight to the continuum between CCSNe types. However, see Valenti et al. (2016) for more on the debate over SNe IIP and IIL and Morozova et al. (2017) for discussion on whether there is a physical process that smoothly gives rise to a continuum between SNe IIP and IIL or whether there is some specific mechanism that more abruptly gives rise to their differences. Type IIb are an intermediate class between SNe II and Ib. They have hydrogen features in their early spectra but these quickly disappear as the SN ages, suggesting a thin hydrogen layer in the progenitor. Liu et al. (2016) showed that there is a continuum of $H\alpha$ strengths between SNe IIb and Ib. Another kind of SN II is the Type IIn, distinguished by its narrow Balmer emission lines that are believed to arise from the SN blast wave colliding with previously ejected progenitor material from stellar winds or eruptions.

SNe II are of interest for several reasons. They mark the deaths of many massive stars and play an important role in the chemical enrichment of the Universe. SNe II light curves and

¹⁰ <http://www.cfa.harvard.edu/supernova/index.html>

¹¹ <https://sne.space/about/>



spectra give insight into SNe II explosion mechanisms and progenitor properties. SNe II also serve as accurate distance indicators. SNe II are not as luminous as SNe Ia (see, for example, Richardson et al. 2002), but they do provide an alternative and independent means of measuring cosmological distances (see, for example, de Jaeger et al. 2017). As more powerful telescopes, such as the Large Synoptic Survey Telescope,¹² observe larger numbers of SNe II at both low and high redshift, SNe II will become more useful cosmological tools than they have been in the past, offering an independent source of distances for calculating the expansion history of the universe. Since most of the SNe observed with large surveys will not be spectroscopically identified, it is important to understand the photometric nature of all types of SNe so that sufficiently pure subsets (e.g., consisting only of SNe Ia or SNe IIP) can be photometrically separated and used for cosmology.

The potential cosmological use of SNe II was pioneered by Kirshner & Kwan (1974, 1975) with the expanding photosphere method (EPM) for measuring distances. The EPM relates the SN II photospheric angular size with the expansion velocity (measured from the spectral lines) in order to calculate the SN's distance (see, for example: Eastman et al. 1996). The EPM does not rely on the extragalactic distance ladder. Schmidt et al. (1992) applied this method to 10 SNe II to calculate their distances and a value for the Hubble constant. Schmidt et al. (1994) improved their method and applied it to 18 SNe II to find a Hubble constant of $H_0 = 73 \pm 6(\text{stat}) \pm 7(\text{syst}) \text{ km s}^{-1} \text{ Mpc}^{-1}$, consistent within the error bars with more recent measurements such as the SN Ia and Cepheid-based value of $H_0 = 73.24 \pm 1.74 \text{ km s}^{-1} \text{ Mpc}^{-1}$ from Riess et al. (2016) and the *Planck* cosmic microwave background radiation-based value of $H_0 = 67.8 \pm 0.9 \text{ km s}^{-1} \text{ Mpc}^{-1}$ from the Planck Collaboration et al. (2016).

More recently, several optical and NIR SN II data sets have been published, while other unpublished data sets have been used for analysis or cosmological applications. We present a summary of many of them and their findings, in largely chronological order. This may also assist anyone interested in compiling SN II data from the literature.

Poznanski et al. (2009) combined optical light curves and spectra of 17 new SN IIP with those of 23 from the literature to find a Hubble diagram dispersion of 0.38 mag, which reduced to 0.22 mag when three $>3\sigma$ outliers were removed. D'Andrea et al. (2010) presented light curves and spectra of 15 SDSS SN IIP and combined them with others from the literature to find a Hubble diagram dispersion of 0.29 mag for the combination.

NIR photometry of SNe II has also been produced and analyzed. Dust extinction at NIR wavelengths is diminished relative to the optical, and there is the additional potential for smaller intrinsic dispersion in NIR light curves of SNe II. Maguire et al. (2010) explain that reduced extinction in the NIR gives rise to a lower error in the extinction estimate and has less of an effect on the fit between expansion velocity and NIR luminosity. They also point out that SN IIP plateau-phase spectra have far fewer lines in the NIR than the optical. They thus presume that estimates of SN IIP NIR luminosity should be less affected by variations in line strengths and line widths between different SN IIP. They examined 12 SN IIP that had spectra and both *VI* and NIR light curves. However, only one

of their SNe was in the Hubble flow ($cz > 3000 \text{ km s}^{-1}$), suggesting the Hubble diagram dispersion they found would be larger than that of Hubble flow objects. In the optical, they found a dispersion of 0.56 mag by combining *V*-band photometry and an estimate of the expansion velocity at +50d post-explosion. In *I*, they found a dispersion of 0.5 mag. Maguire et al. (2010) confirmed their hopes for the NIR by measuring a *J* band dispersion of 0.39 mag, ~ 0.1 mag lower than that in *I*, suggesting that NIR light curves of Hubble-flow SNe II would offer a similar improvement when compared to the optical.

In the past year, Rodríguez et al. (2016) presented preliminary results from a set of 16 SN II, showing a 0.12 mag dispersion Hubble diagram in each of the *JHK_s* bands, better than the *BVI* dispersions of 0.23, 0.17, and 0.19 mag, respectively, providing evidence that the smaller dispersion seen by Maguire et al. (2010) for very-nearby NIR SN II light curves would also be found in the Hubble flow.

More data were published by various groups in the following years. Returning to the optical, Arcavi et al. (2012) produced 21 SN II light curves from the Caltech Core Collapse Project. Taddia et al. (2013) published light curves and spectra of five Carnegie Supernova Project (CSP) SNe IIn. Faran et al. (2014) presented light curves and spectra of 23 SNe IIP from LOSS and analyzed them. Anderson et al. (2014) provided *V*-band light curves and analysis for 116 SN II from the CSP and its predecessors (CT, C&T, SOIRS, and CATS). They found evidence suggesting a continuum, where low-luminosity SN II have flat light curves during the plateau phase and higher-luminosity SN II have faster decline rates. Anderson et al. (2014) measured a dispersion of 0.56 mag around the relation between the plateau-phase decline rate and peak magnitudes, suggesting that SN II can be used as pure photometric distance indicators. Galbany et al. (2016) published all of the bands for 51 of these 116 SN II, while the CSP portion is not yet published. Gutiérrez (2016) presented an in-depth analysis of spectra of 123 SN II from the CSP and its predecessors, finding evidence suggesting that differences between SN IIP and IIL are related to the pre-explosion hydrogen envelope mass and do not come from different progenitor families.

Rodríguez et al. (2014) found a very promising dispersion of 0.12 mag using 13 SN II in the Hubble flow that have a well-constrained shock breakout epoch. González-Gaitán et al. (2015) studied the rise times of 223 SN II light curves from SDSS and SNLS and found evidence that the early light curves of most SN II are powered by cooling of shock-heated ejecta. They also found that massive hydrogen envelopes are indeed needed to explain the plateaus of SN II. Sanders et al. (2015) analyzed 76 multiband Pan-STARRS1 (PS1) SN II light curves and concluded that there does not appear to be two unconnected subclasses of SN II (IIP and IIL), but rather a one-parameter family likely related to the original mass of the progenitor, similar to the findings of Anderson et al. (2014). Sanders et al. (2015) further confirmed that SN IIP appear to be standardizable with an intrinsic dispersion as low as ~ 0.2 mag. Rubin et al. (2016) published 57 *R*-band SN II light curves from the Palomar Transient Factory. Valenti et al. (2016) presented photometry of 12 SN II and combined them with well-sampled light curves from the literature to search for correlations between the slope of the linear light curve decay and other properties.

¹² <http://www.lsst.org/>

Table 1
SN II Discovery Data

SN	Type	Host Galaxy	z_{helio}	Discovery Ref.	Opt LC	NIR LC	# Spectra
SN2000eo	IIn	MCG-2-9-3	0.010347	IAUC 7524	y	...	14
SN2001ez	II	CGCG 329-009 ^a	0.012916	IAUC 7736	y	...	1
SN2001fa	IIn	NGC 673	0.017285	IAUC 7737	y	...	5
SN2002bx	II	IC 2461	0.007539	IAUC 7864	y	...	8
SN2002em	II	UGC 3430	0.013539	IAUC 7955	y	...	0
SN2005ay	II	NGC 3938	0.002699	CBET 128	...	y	4
SN2005kd	IIn	CGCG 327-013 ^a	0.015040	IAUC 8630	y	...	0
SN2006at	II	Anon Gal	0.015000	CBET 424	y	...	1
SN2006be	II	IC 4582	0.007155	CBET 449	y	...	3
SN2006bl	II	MCG +02-40-9	0.032382	CBET 462	y	...	1
SN2006bo	IIn	UGC 11578	0.015347	CBET 468	y	...	0
SN2006bv	IIn	UGC 7848	0.008382	CBET 493	y	...	1
SN2006ca	II	UGC 11214	0.008903	IAUC 8707	y	...	1
SN2006cd	IIP	IC 1179	0.037116	CBET 508	y	...	1
SN2006gy	IIn	NGC 1260	0.019190	CBET 644	y	...	2
SN2006it	IIP	NGC 6956	0.015511	CBET 660	y	...	0
SN2006iw	II	Anon Gal	0.030700	CBET 663	y	...	0
SN2006ov	II	NGC 4303	0.005224	CBET 756	y	...	1
SN2007Q	II	NGC 5888	0.029123	CBET 821	y	...	2
SN2007T	II	NGC 5828	0.013581	CBET 833	y	...	0
SN2007aa	II	NGC 4030	0.004887	CBET 848	y	y	4
SN2007ad	II	UGC 10845	0.027506	CBET 854	y	...	1
SN2007ah	II	UGC 2931	0.019170	CBET 869	y	...	1
SN2007ak	IIn	UGC 3293	0.015634	CBET 875	y	...	0
SN2007av	II	NGC 3279	0.004650	CBET 901	y	y	1
SN2007ay	II	UGC 4310	0.014527	CBET 905	y	...	0
SN2007bb	IIn	UGC 3627	0.020858	CBET 912	y	...	1
SN2007be	II	UGC 7800	0.012515	CBET 917	y	...	1
SN2007bf	II	UGC 9121	0.017769	CBET 919	y	...	1
SN2007cd	II	NGC 5174	0.022799	CBET 950	y	...	0
SN2007ck	II	MCG +05-43-16	0.026962	CBET 970	y	...	1
SN2007cm	IIn	NGC 4644	0.016501	CBET 973	y	...	1
SN2007ct	II	NGC 6944	0.014734	CBET 988	y	...	1
SN2007cu	II ^b	UGC 10214	0.031358	CBET 988	y	...	0
SN2007hv	II	UGC 2858	0.016858	CBET 1056	y	...	1
SN2007od	II	UGC 12846	0.005784	CBET 1116	y	...	13
SN2007pk	IIn	NGC 579	0.016655	CBET 1129	y	...	7
SN2007rt	IIn	UGC 6109	0.022365	CBET 1148	y	y	2
SN2008B	IIn	NGC 5829	0.018797	CBET 1194	y	...	3
SN2008F	IIP	MCG -01-8-15	0.018366	CBET 1207	y	...	1
SN2008aj	IIn	MCG +06-30-34	0.024963	CBET 1259	y	...	1
SN2008bj	II	MCG +08-22-20	0.018965	CBET 1314	y	...	16
SN2008bn	II	NGC 4226	0.024220	CBET 1322	y	...	11
SN2008bu	II	ESO 586-G2	0.022115	CBET 1341	y	...	0
SN2008bx	II	Anon Gal	0.008399	CBET 1348	y	...	3
SN2008gm	IIn	NGC 7530	0.011728	CBET 1549	y	...	1
SN2008if	II	MCG -01-24-10	0.011475	CBET 1619	...	y	1
SN2008in	II	NGC 4303	0.005224	CBET 1636	y	y	13
SN2008ip	IIn	NGC 4846	0.015124	CBET 1641	y	y	11
SN2009K	IIf	NGC 1620	0.011715	CBET 1663	...	y	0
SN2009N	IIP	NGC 4487	0.003456	CBET 1670	y	...	1
SN2009ay	II	NGC 6479	0.022182	CBET 1728	y	y	6
SN2009dd	II	NGC 4088	0.002524	CBET 1764	y	...	9
SN2009kn	IIn	MCG -03-21-6	0.015798	CBET 1997	y	...	4
SN2009kr	II	NGC 1832	0.006468	CBET 2006	...	y	2
SN2010aj	IIP	MCG -01-32-35	0.021185	CBET 2201	y	...	7
SN2010al	Ibn ^c	UGC 4286	0.017155	CBET 2207	y	y	8
SN2010bq	IIn	UGC 10547	0.030988	CBET 2241	y	y	5
SN2011an	IIn	UGC 4139	0.016308	CBET 2668	...	y	2
SN2011ap	IIn	IC 1277	0.023630	CBET 2670	...	y	9

Notes. The SN Type, Host Galaxy, and Discovery Reference columns come from <http://www.cbat.eps.harvard.edu/lists/Supernovae.html>, except as noted. The redshifts, z_{helio} , are of the host galaxy and come from NED, except for 2006at (CBET 441), 2006iw (D'Andrea et al. (2010)), and 2008bx (CBET 1359).

^a Host galaxy from NED.

^b Type from <http://w.astro.berkeley.edu/bait/2007/sn2007cu.html>.

^c Type from Pastorello et al. (2015).

(This table is available in machine-readable form.)

In the past year, de Jaeger et al. (2017) presented a Hubble diagram based on 73 SN II with a redshift range of $0.01 \leq z \leq 0.50$ from the CSP, SDSS, and SNLS and found a Hubble diagram dispersion of 0.35 mag by applying the Photometric Color Method with no redshift information, showing that SNe II can be used as pure photometric distance indicators. On a smaller sample of 61 SNe II and using spectroscopic information, de Jaeger et al. (2017) measured a dispersion of 0.27 mag. Finally, Gall et al. (2017) presented light curves and spectra of nine SNe IIP/L in the redshift range of $0.045 \leq z \leq 0.335$ and combined them with data from the literature to update previous EPM and standardized candle method (SCM) Hubble diagrams. The SCM (Hamuy & Pinto 2002) uses the observed correlation between the luminosity and the expansion velocity of a SN IIP to calculate its distance. An interesting finding is that their three SNe IIL are indistinguishable from their SNe IIP in both the EPM and SCM Hubble diagrams. Larger samples are needed to confirm this, but it suggests that SNe IIL may be useful cosmological distance indicators as well. Given their higher luminosity than SNe IIP, this could make SNe IIL easier to find at higher redshifts, assuming a sufficient observing cadence is used to account for their faster decline.

The Harvard-Smithsonian CfA Supernova Group has been a source of data for nearby SNe since 1993. The primary focus has been SNe Ia, but numerous CCSNe have been observed as well. In addition to various individual SN papers, the CfA1-CfA4 data sets include a total of 345 SN Ia multiband optical light curves (Riess et al. 1999; Jha et al. 2006; Hicken et al. 2009, 2012). Optical spectroscopy of over 400 SNe Ia (Matheson et al. 2008; Blondin et al. 2012) have been published. In the near-infrared, the CfAIR2 set consists of 94 SN Ia light curves (Friedman et al. 2015), with earlier versions of a subset published by Wood-Vasey et al. (2008). The CCSN photometry we acquired up until 2011 was processed along with the SN Ia photometry when the CfA3, CfA4, and CfAIR2 data sets were produced: 61 optical and 25 near-infrared stripped-envelope light curves were presented in Bianco et al. (2014) and 60 SN II/IIn/Iib/Ibn light curves are presented in this work. Two additional NIR light curves have been published elsewhere: SN 2010jl (Fransson et al. 2014) and SN 2011dh (Marion et al. 2014). One SN Iib NIR light curve was produced after Bianco et al. (2014) and it is presented here. Additionally, optical light curves, spectra, and analysis of SN IIP 2005cs and 2006bp were presented in Dessart et al. (2008). Modjaz et al. (2014) presented and analyzed optical spectra of 73 stripped-envelope CCSN, while CfA SN II spectra for 48 of the 60 SN from the current paper are presented here. Finally, the CfA5 data set is currently being produced and will include optical SN light curves of all types taken after the CfA4 era (which included SNe discovered up to mid-2010), plus any earlier ones that were missing calibration or host-galaxy subtraction images when the CfA4 light curves were created. Spectra from the CfA5-era will also be published.

Section 2 describes the data and reduction and Section 3 provides select comparisons of photometry with other data sets for overlapping objects.

2. Data Acquisition and Reduction

The CfA SN II sample consists of 60 objects: 39 SNe II/IIP, 19 IIn, 1 Iib, and 1 that was originally classified as a IIn but later as a Ibn (2010al; see, for example, Pastorello et al. 2015).

Of these, 46 objects have only optical photometry, 6 have only NIR photometry, and 8 have both. The median redshift is 0.016. Optical spectra for 48 of the 60 SNe are presented in this work. See Table 1 for information on each SN's type, host galaxy, redshift, discovery reference, optical or NIR photometry, and number of CfA optical spectra. Most of the SNe were discovered as part of targeted searches.

There are 54 objects in this work with optical photometry: 36 II/IIP, 17 IIn, and 1 Ibn. Measurements were made in the $u'UBVRir'i'$ bands and consist of a total of 2932 light curve points. These data were acquired on the 1.2 m telescope at the FLWO¹³ at the same time as the CfA3 and CfA4 SN Ia data sets. Twenty-six SN II light curves were generated as part of the light curve production process that created the CfA3 set and 28 were generated as part of the process that created the CfA4 set. Five of the CfA3-era SN II light curves were observed on the 4Shooter camera¹⁴ (hereafter referred to as CfA3_{4SH}), and 21 were observed on the KeplerCam¹⁵ (hereafter referred to as CfA3_{KEP}). The 28 CfA4-era SN II light curves (hereafter referred to as CfA4) were all observed on the KeplerCam. Since all of the optical photometry reported here was produced as part of the CfA3 and CfA4 processing campaigns, see Hicken et al. (2009) and Hicken et al. (2012) for greater details on the instruments, observations, photometry pipeline, calibration, and host-galaxy subtraction used to create the CfA SN II light curves. It should be noted that the passbands shifted during part of the CfA4 observing campaign, likely due to deposits or condensation on the KeplerCam, resulting in two sets of color terms for the CfA4 calibration: period 1 color terms before 2009 August 15 (MJD = 55058) and period 2 color terms after. Anyone using the CfA4-era natural-system light curves should be careful to use the appropriate-period passbands, which can be found at our web site.¹⁶ Also, the 1.2 m primary mirror deteriorated during the course of the CfA4 observing, causing a sensitivity loss of about 0.6 mag in V.

There are 14 SNe with NIR photometry in this work: 7 SN II, 5 IIn, 1 Iib, and 1 Ibn. We obtained our JHK_s -band photometry with the robotic 1.3 m Peters Automated InfraRed Imaging TELEscope (PAIRITEL) at FLWO (Bloom et al. 2006). PAIRITEL was a refurbished version of the Two Micron All Sky Survey (2MASS) North telescope using the transplanted 2MASS South camera (Skrutskie et al. 2006). It was utilized from 2005–2013 as a dedicated NIR imager for follow-up of transients, including SN of all types discovered by optical searches (Bloom et al. 2006; Bianco et al. 2014; Friedman et al. 2015). Our NIR observing strategy was described elsewhere (Wood-Vasey et al. 2008; Friedman 2012; Bianco et al. 2014; Friedman et al. 2015). In particular, see Friedman et al. (2015) for a detailed discussion of our image reduction and photometry pipelines, including mosaicking, sky subtraction, and host-galaxy subtraction. Whenever possible, we used an error-weighted mean of light curves derived from multiple host-galaxy template images to remove flux contamination at the SN position. Since PAIRITEL was already on the 2MASS system, the SN brightness in each field was determined with differential photometry using reference field stars from the

¹³ <http://linmax.sao.arizona.edu/FLWO/48/48.html>

¹⁴ <http://linmax.sao.arizona.edu/FLWO/48/OLD/4shccd.html>

¹⁵ <http://linmax.sao.arizona.edu/FLWO/48/kepcdd.html>

¹⁶ <http://www.cfa.harvard.edu/supernova/index.html>

Table 2
Journal of Spectroscopic Observations

SN	MJD	Tel./Instr. ^a	Range (Å)	Disp (Å/pix)	Airmass	Exp. (s)
SN2007aa	54154.484	FAST	3556–7455	1.46	1.48	1200
SN2007aa	54156.392	FAST	3477–7413	1.47	1.19	1500
SN2007aa	54169.360	FAST	3479–7417	1.47	1.20	1200
SN2007aa	54185.372	FAST	3476–7418	1.47	1.33	1500
SN2007ad	54154.528	FAST	3555–7454	1.46	1.11	1500
SN2007ah	54171.158	FAST	3478–7414	1.47	1.49	1800
SN2007av	54184.324	FAST	3478–7414	1.47	1.21	1200
SN2007bb	54198.157	FAST	3474–7416	1.47	1.19	1800
SN2007be	54201.295	FAST	3477–7413	1.47	1.18	1800
SN2007bf	54201.327	FAST	3477–7413	1.47	1.05	1800
SN2007ck	54243.376	FAST	3477–7413	1.47	1.01	1800

Note. It is also available at the CfA web site: <http://www.cfa.harvard.edu/supernova/index.html>.

^a Telescope and instrument used for this spectrum: FAST: FLWO1.5m+FAST; MMTblue: MMT+Blue Channel

(This table is available in its entirety in machine-readable form.)

2MASS point source catalog (Cutri et al. 2003). There are a total of 816 NIR light curve points.

Of our 14 NIR light curves, 11 had host-galaxy subtraction as described in Friedman et al. (2015), while 3 objects were sufficiently isolated from the host-galaxy nucleus (SN 2010bq, SN 2011an, SN 2011ap) and forced DoPHOT photometry (Schechter et al. 1993) was used at the SN position without template image subtraction. The optical light curve of SN 2009K was presented in Bianco et al. (2014) but the NIR light curve did not have final calibration and host-galaxy images, so it is presented here.

We acquired 195 optical spectra for 48 of the 60 SNe in this work. Spectra were obtained using the FLWO 1.5 m Tillinghast telescope with the FAST spectrograph (Fabricant et al. 1998) and the MMT Telescope with the Blue Channel Spectrograph. The FAST spectra were taken using a 3" slit with an atmospheric corrector, with typical FWHM resolution of 6–7 Å. The observations at the MMT were taken with a 1" slit and a 300 line/mm grating at the parallactic slit position, also with a typical FWHM resolution of 6–7 Å. All Spectra were reduced and flux-calibrated by a combination of standard IRAF and custom IDL procedures (Matheson et al. 2005). The 2D spectra underwent flat-fielding, cosmic-ray removal, and extraction into 1D spectra, consisting of flux and flux error measurements. Pairs of spectroscopic standard stars were obtained to provide flux calibration (with no second-order contamination) and assist in the removal of telluric features. For more detail, see Matheson et al. (2008) and Blondin et al. (2012). The journal of observations of the spectra is in Table 2.

2.1. Star Sequences, Light Curves, and Spectra

In Table 3 we present the standard-system optical star sequences for the CfA SN II photometry and in Tables 4 and 5 we present the natural-system and standard-system optical light curves, respectively. Standard system photometry places (or attempts to place) photometric measurements in a well-defined and standard passband, whereas natural-system photometry leaves the measurements in the detector's passband. We observed standard stars as described in Hicken et al. (2009) and Hicken et al. (2012) on photometric nights to calculate photometric solutions (including zeropoints and color terms)

and applied those solutions to field stars around each SN to create the standard-system optical star sequences. We created the natural-system optical star sequences by applying the very same photometric solutions, except without the color terms. We then used these natural-system star sequences to calibrate each SN's natural-system optical light curve. The SN standard-system light curves were derived by applying the color terms to the SN natural-system light curve, but we caution the reader that using star-derived color terms for placing SN light curves on the standard system is not highly accurate and they were created primarily to allow quick and rough comparisons with other SN photometry. No S-corrections were performed. For most uses, we recommend the reader use the natural-system light curves that we present.

Note the seven CfA3-era SN II optical light curves that were well-removed from their host galaxies and did not require host-galaxy subtraction. They can be identified in Tables 4 and 5 as those that have $N_{\text{host}} = 0$ host subtractions. The rest of the CfA3-era SN II light curves have $N_{\text{host}} = 1$. All of the CfA4-era light curves were host-subtracted and have $N_{\text{host}} \geq 1$. We remind the reader that the CfA4 period-1 and period-2 natural-system passbands are different, so special care should be taken to use the correct period-1 or period-2 passband for the natural-system CfA4-era SN II light curves for each point. In the last column of Table 4, KEP1 means it was taken on the KeplerCam during CfA4 period 1 and KEP2 signifies period 2. CfA4-era data before 2009 August 15 (MJD = 55058) is period 1 and CfA4-era data after is period 2.

The CfA4 Ia light curves (Hicken et al. 2012) and the CfA4-era SN II light curves in this work were created at the same time following the same procedures. They usually had multiple host subtractions for each light curve data point, giving rise to multiple values and uncertainties for each data point. The median of the multiple values for the CfA4-era light curves, which arise from the multiple subtractions for each data point, was chosen to be the light curve value for that date. The uncertainty for the CfA4-era light curves was created from two components: the median of the photometric pipeline uncertainties for each light curve point was added in quadrature to the standard deviation of the multiple host-subtraction light curve values for that point. However, the CfA3-era light curves in this work did not have multiple

Table 3
Standard-system Star Sequences

SN	Star	R.A.(J2000)	Decl.(J2000)	V	N_V	$U - B$	N_U	$B - V$	N_B	$V - r$	N_r	$V - i$	N_i
SN2007aa	01	12:00:38.638	-01:06:55.25	16.213(0.014)	2	...	0	1.238(0.058)	2	0.538(0.023)	2	1.043(0.023)	2
SN2007aa	02	12:00:36.905	-01:05:53.67	17.245(0.016)	2	...	0	0.556(0.021)	2	0.149(0.009)	2	0.285(0.011)	2
SN2007aa	03	12:00:35.217	-01:03:51.48	17.324(0.026)	2	...	0	0.648(0.055)	2	0.197(0.037)	2	0.366(0.011)	2
SN2007aa	04	12:00:25.058	-01:02:49.29	17.802(0.030)	2	...	0	0.625(0.044)	2	0.124(0.027)	2	0.334(0.023)	2
SN2007aa	05	12:00:24.144	-01:09:55.72	17.359(0.014)	2	...	0	0.533(0.032)	2	0.138(0.011)	2	0.276(0.009)	2
SN2007aa	06	12:00:20.107	-01:06:22.99	17.451(0.029)	2	...	0	0.527(0.039)	2	0.306(0.068)	2	0.436(0.030)	2
SN2007aa	07	12:00:19.767	-01:05:03.02	15.299(0.012)	2	...	0	0.615(0.019)	2	0.161(0.018)	2	0.308(0.022)	2
SN2007aa	08	12:00:16.229	-01:02:14.43	17.954(0.033)	2	...	0	0.736(0.047)	2	0.246(0.013)	2	0.504(0.010)	2
SN2007aa	09	12:00:14.168	-01:04:24.72	17.185(0.016)	2	...	0	0.636(0.017)	2	0.177(0.017)	2	0.325(0.009)	2
SN2007aa	10	12:00:08.517	-01:07:18.48	15.374(0.015)	2	...	0	1.406(0.022)	2	0.574(0.014)	2	1.255(0.011)	2
SN2007aa	11	12:00:07.955	-01:04:42.70	16.902(0.020)	2	...	0	1.349(0.018)	2	0.555(0.012)	2	1.085(0.012)	2
SN2007aa	12	12:00:07.616	-01:04:57.01	16.756(0.012)	2	...	0	0.685(0.015)	2	0.196(0.022)	2	0.357(0.009)	2

Note. The V magnitudes and the colors of the stars are presented, along with the number of nights of calibration in each band: N_V , N_U , N_B , etc. The generic letters r and i are used in the final four column headers and should be interpreted as the R and I bands, respectively, for SN 2000eo, 2001ez, 2001fa, 2002bx, and 2002em and as the r' and i' bands, respectively, for the rest. This information is also available at the CfA web site: <http://www.cfa.harvard.edu/supernova/index.html>.

(This table is available in its entirety in machine-readable form.)

Table 4
Natural-system SN Light Curves

SN	Filter	MJD	N_{host}	Mag	σ	Production Campaign	Camera
SN2007aa	B	54152.35648	0	16.167	0.016	CfA3	KEP
SN2007aa	B	54153.32938	0	16.226	0.017	CfA3	KEP
SN2007aa	V	54152.35348	0	15.703	0.012	CfA3	KEP
SN2007aa	V	54153.32638	0	15.719	0.013	CfA3	KEP
SN2007aa	r'	54152.35117	0	15.571	0.013	CfA3	KEP
SN2007aa	r'	54153.32407	0	15.580	0.014	CfA3	KEP
SN2007aa	i'	54152.34885	0	15.694	0.012	CfA3	KEP
SN2007aa	i'	54153.32176	0	15.717	0.015	CfA3	KEP
SN2009N	B	54857.50559	5	16.398	0.022	CfA4	KEP1
SN2009N	B	54858.55471	5	16.401	0.024	CfA4	KEP1
SN2009N	V	54857.51825	9	16.294	0.020	CfA4	KEP1
SN2009N	V	54858.55843	5	16.303	0.023	CfA4	KEP1
SN2009N	r'	54857.51585	4	16.272	0.028	CfA4	KEP1
SN2009N	r'	54858.54485	5	16.261	0.016	CfA4	KEP1
SN2009N	i'	54857.50628	8	16.192	0.027	CfA4	KEP1
SN2009N	i'	54858.54786	5	16.159	0.015	CfA4	KEP1

Note. This table presents the CfA natural-system SN II photometry. N_{host} is the number of host-galaxy images subtracted from the same data image. $N_{\text{host}} = 0$ means no host-galaxy subtraction was performed and the SN was sufficiently removed from the host galaxy. σ is the same as the light curve uncertainty used in Hicken et al. (2009) and is the same as σ_{pipe} in Hicken et al. (2012). The penultimate column lists during which light curve production campaign that data point was produced: CfA3 or CfA4. The last column lists which camera the SN data was acquired with. For CfA4 data, a 1 or 2 is appended to “KEP” to indicate if it was taken during period 1 or 2 and which set of natural-system bandpasses should be used. Only the first two nights in each band of two SN (one from CfA3 and one from CfA4) are shown here for guidance regarding its form and content. This information is also available at the CfA web site, as are the natural-system passbands: <http://www.cfa.harvard.edu/supernova/index.html>.

(This table is available in its entirety in machine-readable form.)

host-galaxy subtractions, thus their uncertainty consists only of the photometric pipeline uncertainty. To ensure that the CfA3-era and CfA4-era SN II light curve uncertainties in this work are comparable, we chose to only use the median of the photometric pipeline uncertainties for the CfA4-era SN II light curves (as opposed to adding it in quadrature to the standard deviation of the multiple subtraction light curve values for a given data point).

In Table 6 we present the PAIRITEL NIR light curves. Figures 1 and 2 show two examples of CfA SN II light curves: one optical (SN 2008bn) and one with both optical and NIR (SN 2008in). Figure 3 shows the spectral series of SN 2007pk, a II_n, and SN 2008bn, a IIP. The photometry and spectra are

available from the journal, the CfA SN Group web site,¹⁷ and The Open Supernova Catalog.¹⁸ The natural-system passbands mentioned in Hicken et al. (2012) are also available at our web site. The period-1 passbands can be used for the CfA3 KeplerCam and the CfA4 period-1 natural-system light curves, while the period-2 passbands can be used for the CfA4 period-2 natural-system light curves. The 4Shooter natural-system passbands can be found in Jha et al. (2006) for use with the CfA3 4Shooter natural-system light curves.

¹⁷ <http://www.cfa.harvard.edu/supernova/index.html>

¹⁸ <https://sne.space/about/>

Table 5
Standard-system SN Light Curves

SN	Filter	MJD	N_{host}	Mag	σ
SN2007aa	B	54152.35648	0	16.197	0.016
SN2007aa	B	54153.32938	0	16.259	0.017
SN2007aa	B	54158.34955	0	16.378	0.021
SN2007aa	B	54158.36546	0	16.371	0.022
SN2007aa	B	54169.35950	0	16.552	0.018
SN2007aa	V	54152.35348	0	15.694	0.012
SN2007aa	V	54153.32638	0	15.709	0.013
SN2007aa	V	54158.34654	0	15.720	0.013
SN2007aa	V	54158.36245	0	15.729	0.012
SN2007aa	V	54159.46133	0	15.704	0.014
SN2007aa	r'	54152.35117	0	15.568	0.013
SN2007aa	r'	54153.32407	0	15.576	0.014
SN2007aa	r'	54158.34423	0	15.563	0.013
SN2007aa	r'	54158.36015	0	15.572	0.015
SN2007aa	r'	54159.45900	0	15.557	0.014
SN2007aa	i'	54152.34885	0	15.685	0.012
SN2007aa	i'	54153.32176	0	15.707	0.015
SN2007aa	i'	54158.34190	0	15.647	0.015
SN2007aa	i'	54158.35785	0	15.644	0.014
SN2007aa	i'	54159.45671	0	15.622	0.015

Note. This table presents the CfA standard-system SN II photometry. N_{host} is the number of host-galaxy images subtracted from the same data image. $N_{\text{host}} = 0$ means no host-galaxy subtraction was performed and the SN was sufficiently removed from the host galaxy. σ is the same as the light curve uncertainty used in Hicken et al. (2009) and is the same as σ_{pipe} in Hicken et al. (2012). Only the first five nights in each band of one SN are shown here for guidance regarding its form and content. This information is also available at the CfA web site: <http://www.cfa.harvard.edu/supernova/index.html>.

(This table is available in its entirety in machine-readable form.)

Table 6
NIR Natural-system SN Light Curves

SN	Filter	MJD	Mag	σ
SN2005ay	J	53480.15	14.513	0.011
SN2005ay	J	53481.21	14.513	0.027
SN2005ay	J	53482.17	14.461	0.022
SN2005ay	J	53486.18	14.455	0.013
SN2005ay	J	53488.17	14.529	0.044
SN2005ay	H	53480.15	14.319	0.034
SN2005ay	H	53481.21	14.474	0.034
SN2005ay	H	53482.17	14.437	0.027
SN2005ay	H	53486.18	14.278	0.018
SN2005ay	H	53487.17	14.252	0.022
SN2005ay	K_s	53480.15	14.177	0.022
SN2005ay	K_s	53481.21	14.208	0.035
SN2005ay	K_s	53482.17	14.196	0.031
SN2005ay	K_s	53486.18	14.102	0.015
SN2005ay	K_s	53487.17	14.188	0.018

Note. This table presents the CfA NIR natural-system SN II photometry. Only the first five nights in each band of one SN are shown here for guidance regarding its form and content. This information is also available at the CfA web site: <http://www.cfa.harvard.edu/supernova/index.html>.

(This table is available in its entirety in machine-readable form.)

3. Photometry Comparison with Other Samples

We compared the $BVR'i'$ CfA SN II star sequences and light curves with overlapping data from two other groups and found

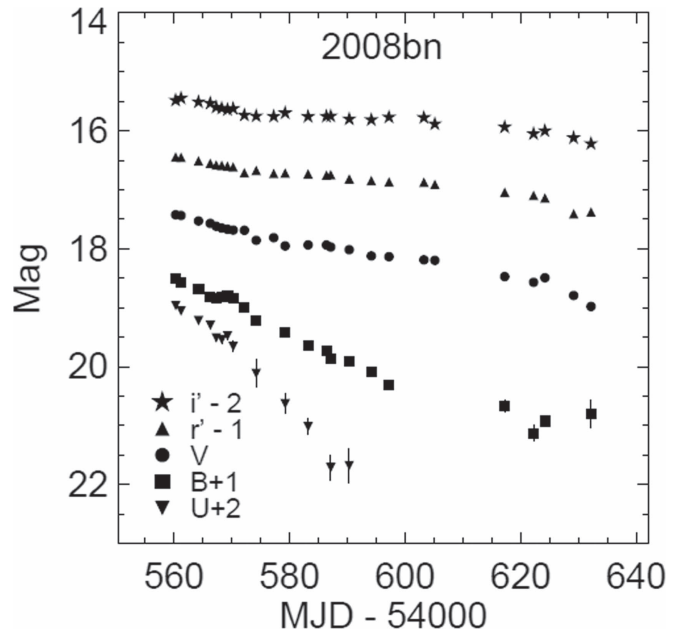


Figure 1. Optical light curves of SN 2008bn. Most error bars are smaller than the symbols.

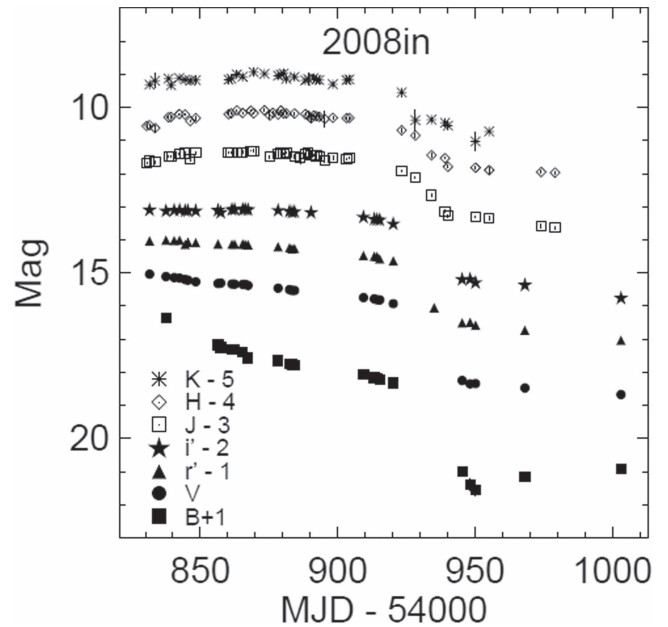


Figure 2. Optical and NIR light curves of SN 2008in. Most error bars are smaller than the symbols.

reasonable agreement overall, although a few objects have larger discrepancies.

3.1. Comparison of CfA and Pan-STARRS1 Star Sequences

Scolnic et al. (2015) (S15) introduced the Supercal method, which provides a very useful analysis tool to estimate systematic photometric offsets among many of the SN Ia samples, including those from the CfA. Their work enables the different samples to be placed much more reliably on one photometric system. For anyone combining SN II samples from various groups and needing to put them on one system, we recommend that either the offsets from S15 be applied for photometric systems covered by

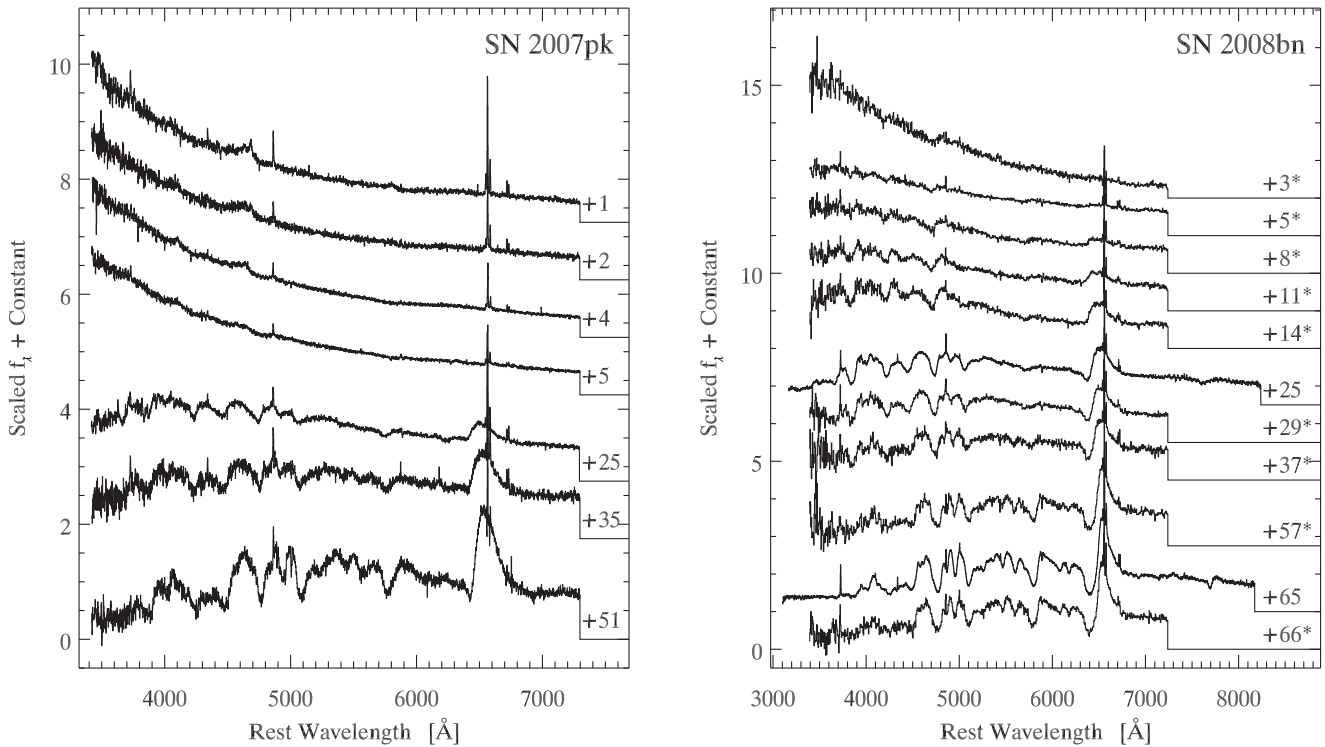


Figure 3. Examples of SN II spectral series from the CfA SN Group. The flux units are f_λ ($\text{erg s}^{-1} \text{cm}^{-2} \text{\AA}^{-1}$) that have been normalized and then had additive offsets applied for clarity. The zero-flux level for each spectrum is marked with an extension on the red edge. The wavelength axis is corrected for the recession velocity of the host galaxy. The number associated with each spectrum indicates the age in (rest-frame) days from the date of discovery. Spectra with low S/N have been binned to 5\AA per pixel; they are indicated with an asterisk appended to the age label. Shown are spectra of a Type IIp (SN 2007pk) and a Type IIc (SN 2008bn). The data used to create this figure are available.

Table 7
Comparison of CfA SN II Star Sequences with Pan-STARRS1 by CfA Subsample

Sample	$\langle \Delta B \rangle_w$ (mmag)	$\langle \Delta V \rangle_w$ (mmag)	$\langle \Delta r' \rangle_w$ (mmag)	$\langle \Delta i' \rangle_w$ (mmag)
CfA SN II stars–PS1 (all matches)	-17.5 ± 1.4	1.0 ± 0.8	12.3 ± 1.0	-14.1 ± 1.1
CfA3 _{4SH} SN II stars–PS1	-24.9 ± 6.9	-0.4 ± 4.6
S15 CfA3 _{4SH} –PS1	-34.5 ± 5.3	1.8 ± 3.8
CfA3 _{KEP} SN II stars–PS1	-11.8 ± 3.6	12.3 ± 2.2	25.1 ± 2.8	0.0 ± 2.8
S15 CfA3 _{KEP} –PS1	-30.9 ± 5.3	2.6 ± 3.6	12.4 ± 3.5	0.8 ± 3.6
CfA4 _{KEP} SN II stars–PS1	-18.2 ± 1.6	-0.8 ± 0.9	10.3 ± 1.1	-16.5 ± 1.2
S15 CfA4 ₁ –PS1	-20.1 ± 5.7	4.5 ± 3.6	4.9 ± 3.3	-0.8 ± 3.6
S15 CfA4 ₂ –PS1	5.2 ± 6.4	5.1 ± 3.7	9.0 ± 3.4	-1.4 ± 3.6

Note. This table presents the weighted mean of the difference between standard-system CfA and Pan-STARRS1 matched stars (CfA minus PS1) in $BVr'i'$ for the whole CfA SN II sample and for the subsamples listed, subject to the luminosity and color restrictions mentioned in the text. Below each subsample's line from this work is the S15 NGSL offset to serve as a rough comparison. However, note that the quantities from this work and S15 are not directly comparable since they are different things, nor are they based on the same sample of stars, so any similarity or difference is more suggestive than conclusive. Also, note that the signs for the S15 NGSL differences are reversed here since the order of subtraction is CfA minus PS1 here, vs. PS1 minus CfA in S15.

S15 or that the general method be followed to calculate offsets for photometric systems not covered.

To check how accurate our star sequence calibrations are, we did not apply the Supercal method but simply compared our standard-system star photometry with the recently released Pan-STARRS1 (PS1) Catalog,¹⁹ converted to the standard system. Using the coordinates for each of the stars from

Table 3, we searched the PS1 catalog. We required a separation of 0.5 arc seconds or less for a match. We added the offsets from Table 3 of Scolnic et al. (2015) to transform the PS1 catalog values (which have the calibration of S15) to the Tonry et al. (2012) calibration. We then applied the transformation equations of Table 6 of Tonry et al. (2012) to convert to the standard-system $BVri$. Finally, we converted from SDSS²⁰ ri to

¹⁹ <http://archive.stsci.edu/panstarrs/search.php?form=fuf>

²⁰ http://classic.sdss.org/dr7/algorithms/jeg_photometric_eq_dr1.html

Table 8
Comparison of CfA SN II Star Sequences with Pan-STARRS1 by SN

SN	$\langle \Delta B \rangle_w$ (mag)	N	$\langle \Delta V \rangle_w$ (mag)	N	$\langle \Delta r' \rangle_w$ (mag)	N	$\langle \Delta i' \rangle_w$ (mag)	N
SN2001ez	-0.059 ± 0.023	10	-0.034 ± 0.016	10	
SN2001fa	-0.028 ± 0.030	10	0.004 ± 0.021	10	
SN2002bx	0.014 ± 0.021	8	0.020 ± 0.014	8	
SN2002em	-0.026 ± 0.008	11	0.000 ± 0.005	11	
SN2004et	-0.007 ± 0.008	8	0.014 ± 0.005	8	0.016 ± 0.005	8	-0.002 ± 0.005	8
SN2005kd	-0.074 ± 0.008	9	-0.002 ± 0.005	9	0.023 ± 0.006	9	-0.009 ± 0.006	9
SN2006at	-0.014 ± 0.030	4	-0.011 ± 0.020	4	0.027 ± 0.027	4	-0.002 ± 0.027	4
SN2006be	0.026 ± 0.026	5	0.031 ± 0.017	5	0.065 ± 0.023	5	0.030 ± 0.024	5
SN2006bl	-0.015 ± 0.006	18	0.001 ± 0.004	18	0.015 ± 0.005	18	-0.014 ± 0.005	18
SN2006bo	-0.001 ± 0.026	6	-0.019 ± 0.018	6	-0.001 ± 0.023	6	-0.050 ± 0.024	6
SN2006bv	-0.023 ± 0.026	6	-0.008 ± 0.018	6	0.020 ± 0.023	6	-0.014 ± 0.024	6
SN2006ca	-0.013 ± 0.050	1	-0.029 ± 0.035	1	-0.017 ± 0.045	1	-0.052 ± 0.047	1
SN2006cd	-0.004 ± 0.023	6	-0.008 ± 0.016	6	0.026 ± 0.021	6	-0.002 ± 0.021	6
SN2006gy	-0.028 ± 0.004	38	-0.012 ± 0.002	38	-0.008 ± 0.003	38	-0.059 ± 0.003	38
SN2006it	-0.007 ± 0.005	27	-0.019 ± 0.003	27	-0.009 ± 0.004	27	-0.050 ± 0.006	27
SN2006iw	-0.024 ± 0.048	2	-0.003 ± 0.034	2	0.016 ± 0.043	2	0.003 ± 0.045	2
SN2006ov	-0.095 ± 0.035	1	0.023 ± 0.014	1	0.024 ± 0.017	1	-0.021 ± 0.017	1
SN2007Q	0.066 ± 0.027	7	0.030 ± 0.018	7	0.043 ± 0.024	7	-0.004 ± 0.025	7
SN2007T	0.117 ± 0.022	8	0.092 ± 0.015	8	0.088 ± 0.020	8	0.052 ± 0.020	8
SN2007aa	-0.011 ± 0.023	3	0.009 ± 0.015	3	0.023 ± 0.017	3	-0.005 ± 0.015	3
SN2007ad	-0.035 ± 0.047	3	-0.025 ± 0.033	3	-0.034 ± 0.042	3	-0.030 ± 0.044	3
SN2007ah	-0.014 ± 0.008	11	-0.013 ± 0.005	11	0.001 ± 0.005	11	-0.038 ± 0.005	11
SN2007av	-0.012 ± 0.009	7	0.021 ± 0.006	7	0.018 ± 0.011	7	-0.008 ± 0.011	7
SN2007bb	0.138 ± 0.026	5	0.111 ± 0.018	5	0.104 ± 0.023	5	0.048 ± 0.024	5
SN2007be	-0.013 ± 0.023	8	0.029 ± 0.016	8	0.046 ± 0.021	8	0.028 ± 0.021	8
SN2007bf	-0.022 ± 0.027	9	0.015 ± 0.018	9	0.043 ± 0.024	9	0.038 ± 0.025	9
SN2007cd	0.003 ± 0.023	8	0.035 ± 0.016	8	-0.057 ± 0.021	8	-0.073 ± 0.021	8
SN2007ck	0.008 ± 0.010	12	0.004 ± 0.005	12	0.032 ± 0.006	12	0.010 ± 0.007	12
SN2007cm	0.041 ± 0.027	1	0.053 ± 0.016	1	0.078 ± 0.017	1	0.059 ± 0.017	1
SN2007ct	0.032 ± 0.011	37	0.038 ± 0.006	37	0.048 ± 0.008	37	0.015 ± 0.007	37
SN2007cu	0.022 ± 0.014	7	0.036 ± 0.007	7	0.054 ± 0.009	7	0.032 ± 0.009	7
SN2007hv	-0.053 ± 0.006	23	-0.003 ± 0.003	23	0.010 ± 0.004	23	-0.042 ± 0.004	23
SN2007od	-0.000 ± 0.031	3	-0.007 ± 0.022	3	0.030 ± 0.028	3	0.010 ± 0.028	3
SN2007pk	-0.034 ± 0.010	20	-0.013 ± 0.005	20	-0.001 ± 0.008	20	-0.029 ± 0.008	20
SN2007rt	-0.001 ± 0.011	6	0.014 ± 0.006	6	0.032 ± 0.008	6	0.011 ± 0.009	6
SN2008aj	-0.014 ± 0.014	4	-0.008 ± 0.007	4	0.010 ± 0.009	4	-0.011 ± 0.009	4
SN2008B	-0.008 ± 0.026	4	0.015 ± 0.014	4	0.055 ± 0.017	4	0.041 ± 0.018	4
SN2008F	0.036 ± 0.013	7	0.038 ± 0.007	7	0.051 ± 0.009	7	0.024 ± 0.009	7
SN2008bj	0.006 ± 0.010	6	0.028 ± 0.007	6	0.054 ± 0.008	6	0.018 ± 0.008	6
SN2008bn	-0.026 ± 0.010	7	0.001 ± 0.006	7	0.021 ± 0.007	7	0.004 ± 0.007	7
SN2008bu	-0.077 ± 0.006	17	-0.023 ± 0.004	17	-0.040 ± 0.005	17	-0.042 ± 0.005	17
SN2008bx	-0.031 ± 0.011	11	0.016 ± 0.006	11	0.033 ± 0.007	11	0.003 ± 0.007	11
SN2008gm	-0.023 ± 0.010	6	-0.008 ± 0.006	6	0.009 ± 0.007	6	-0.027 ± 0.007	6
SN2008in	-0.057 ± 0.013	4	-0.018 ± 0.008	4	0.023 ± 0.010	4	-0.019 ± 0.009	4
SN2008ip	-0.015 ± 0.012	5	0.011 ± 0.007	5	0.034 ± 0.008	5	0.019 ± 0.008	5
SN2009ay	-0.013 ± 0.007	14	-0.002 ± 0.004	14	0.011 ± 0.005	14	-0.006 ± 0.005	14
SN2009dd	-0.024 ± 0.032	1	0.014 ± 0.027	1	0.048 ± 0.020	1	0.020 ± 0.017	1
SN2009kn	-0.001 ± 0.005	42	0.005 ± 0.003	42	0.011 ± 0.004	42	-0.005 ± 0.004	42
SN2009N	-0.019 ± 0.013	4	0.001 ± 0.008	4	0.011 ± 0.010	4	-0.010 ± 0.010	4
SN2010aj	-0.016 ± 0.014	4	0.003 ± 0.008	4	0.029 ± 0.010	4	0.019 ± 0.010	4
SN2010al	-0.009 ± 0.006	19	0.006 ± 0.004	19	0.025 ± 0.004	19	0.015 ± 0.004	19

Note. This table presents the weighted mean of the difference between standard-system CfA and PS1 stars (CfA minus PS1) in $BVr'i'$ for each individual SN's star sequence and how many stars were matched. 50 CfA SN II have star matches with PS1 after luminosity and color restrictions. Four SN star sequences have no PS1 matches. Additionally, we calibrated a star sequence for SN 2004et on the KeplerCam and include it in this analysis even though the light curve is not available.

Smith et al. (2002) $r'i'$, though there is minimal difference. Similar to S15, we removed PS1 stars brighter than 14.8, 14.9, and 15.1 mag in gri to avoid saturated stars and used the broader of the two S15 color ranges ($0.3 < g - i < 1.0$) in order to have more stars to compare with. After applying these conditions, 50 of the 54 CfA SN II optical star sequences still

had some stars in common with the PS1 Catalog. Additionally, we had a star sequence (but no light curve) for SN 2004et that we compared with PS1, bringing the number of star sequences compared with PS1 to 51.

The weighted means of the CfA-minus-PS1 matched-star differences are shown in Table 7 for the CfA SN II sample as a

Table 9
Comparison of CfA SN II Star Sequences with CSP by SN

SN	$\langle\Delta B\rangle$ (mag)	N	$\langle\Delta V\rangle$ (mag)	N	$\langle\Delta r'\rangle$ (mag)	N	$\langle\Delta i'\rangle$ (mag)	N
SN2006be	0.004	5	0.036	5	0.058	4	0.036	5
SN2006bl	-0.016	13	0.002	13	0.015	13	0.002	13
SN2006bo	-0.023	4	-0.017	4	-0.083	4	-0.017	4
SN2006it	-0.025	12	-0.015	12	-0.019	12	-0.015	12
SN2007aa	0.016	10	0.017	10	0.043	10	0.017	10
SN2007od	-0.018	6	-0.015	6	-0.014	6	-0.015	6
SN2008bu	-0.006	9	0.019	9	0.024	9	0.019	9
SN2009N	0.029	8	0.039	8	0.051	7	0.039	8

Note. This table presents the average of the difference between standard-system CfA and CSP stars (CfA minus CSP) in $BVr'i'$ for 8 individual SN star sequences and how many stars were matched.

Table 10
Comparison of CfA SN II Light Curves with CSP by SN

SN	Band	$\langle\Delta \text{mag}\rangle$	N
SN2006bo	B	-0.027	3
SN2006bo	V	-0.046	4
SN2006bo	r'	-0.033	4
SN2006bo	i'	-0.011	4
SN2006be	V	0.071	7
SN2006bl	V	0.106	5
SN2006it	V	-0.038	1
SN2007aa	V	-0.010	5
SN2007od	V	-0.015	6
SN2008bu	V	-0.033	1
SN2009N	V	0.032	1

Note. This table presents the average of the difference between standard-system CfA and CSP light curve points for eight SNe (CfA minus CSP, with $\Delta\text{MJD} < 0.6$ days), in $BVr'i'$ for 2006bo and V for the other seven, and how many light curve points were matched.

whole, and for the separate CfA_{3_{SH}}, CfA_{3_{KEP}}, and CfA4 matched-star subsamples. No effort was made to convert the CfA_{3_{SH}} RI bands into ri and so only BV comparisons are available for CfA_{3_{SH}} stars. The weighted-average differences of all the stars combined for the respective $BVr'i'$ bands are -0.018 , 0.001 , 0.012 , and -0.014 mag.

In this work, the CfA B calibration is about 0.02 brighter, in the same direction found by S15 in their Table 4 (NGSL column). It should be noted that the comparisons of this work and S15 are not the same. First of all, the star sequences in S15 are different from those in this work. More importantly, S15 used observed natural-system and synthetic natural-system photometry, while this work is using standard-system photometry, so any similarities or differences in the values between the two works' offsets are not conclusive but merely suggestive.

In this work, CfA V has virtually no offset with the PS1 conversion to V for the CfA_{3_{SH}} and CfA4 subsamples, in rough agreement with S15. However, the CfA_{3_{KEP}} subsample is 0.012 mag fainter, about 0.01 mag fainter than the offset S15 found.

CfA r' is fainter than PS1 in this work, as is the case in S15, though the offset here is greater than in S15. There is excellent agreement between the CfA_{3_{KEP}} i' offsets in the two works but the CfA4 i' offset in this work is 0.0165 mag brighter, while there is virtually no offset in S15.

With the exception of CfA_{3_{KEP}} V and CfA4 i' , there is reasonable directional agreement in the CfA-minus-PS1 offsets of this work and S15, in the sense of both agreeing on which calibration is fainter or brighter.

On a SN-by-SN basis, Table 8 shows the weighted mean of the CfA-minus-PS1 star differences for each CfA SN II that had matches. Of the 51 SNe II, 19 (37%) have V offsets within ± 0.01 mag, 34 (67%) have V offsets within ± 0.02 mag, 42 (82%) have offsets within ± 0.03 mag, and 48 (94%) have offsets within ± 0.038 mag. These can be considered to have reasonable agreement with PS1. However, there are 3 SNe with larger calibration discrepancies. SN 2007bb has a V offset of 0.111 mag based on 5 matched stars, SN 2007T has a 0.092 mag offset based on 8 stars, and SN 2007cm has a 0.053 mag offset based on only 1 star.

3.2. Comparison of CfA and CSP Star Sequences and SN II Light Curves

The CSP provided us with standard-system $BVr'i'$ star sequences for their upcoming SN II light curve publication (C. Contreras 2017, private communication). Table 9 shows the $BVr'i'$ comparisons between 8 CfA and CSP star sequences, with the average of the differences in V ranging from -0.017 to 0.039 mag, showing reasonable agreement. However, we point out a larger difference of -0.083 mag in r' for SN 2006bo.

We also took the CSP natural-system V light curves for 7 objects from Anderson et al. (2014) and the natural-system $BVr'i'$ light curves for SN 2006bo from Taddia et al. (2013) and applied color terms²¹ to convert them to the standard system and compare with the CfA standard-system light curves from Table 5. Applying star-derived color terms to SN photometry to create standard-system light curves is fraught with danger and inaccuracy (the user is encouraged to use the natural-system light curves whenever possible), so this is intended only as a rough comparison and sanity check. Only points that are within 0.6 days of each other are matched. No interpolation was used to provide for more points of comparison. Table 10 shows the average of the light curve differences for the 8 SN II in common (11 comparisons in total: 8 in V and 1 in each of $Br'i'$). Of the 11 comparisons, 8 are within ± 0.04 mag, while one has CfA 0.046 mag brighter, another has CfA 0.071 mag fainter, and the most disparate one has CfA 0.106 mag fainter. This is comparable to the similarity that the CfA3 and CfA4 SN Ia light curves had

²¹ $CT_B = +0.069$, $CT_V = -0.063$, $CT_{r'} = -0.016$, $CT_{i'} = 0.0$ (Stritzinger et al. 2011, and C. Contreras 2017, private communication).

with other groups' light curves in Hicken et al. (2009) and Hicken et al. (2012), and suggests that the CfA SN II light curves are of reasonable accuracy.

4. Conclusion

The CfA SN II light curve sample consists of 60 multiband light curves: 46 have only optical, 6 have only NIR, and 8 have both optical and NIR. We also present 195 optical spectra for 48 of the 60 SNe. This work includes a total of 2932 optical and 816 NIR light curve points. There are 26 optical and 2 NIR light curves of SNe II/IIP with redshifts $z > 0.01$, some of which may give rise to useful distances for Hubble diagrams. Select comparisons with other groups' data show reasonable agreement in the vast majority of cases. These light curves add to a growing body of SN II data from the literature. This collective body of data (from the literature, this work, and future samples) will be useful for providing greater insight into SN II explosions, developing analytic methods for photometric SN classification, and opening the path for their increasing use as cosmological distance indicators. Having another method for measuring the expansion history of the Universe, independent from SNe Ia, will serve the important purpose of either confirming the results derived from SNe Ia or offering insights for improving the cosmological use of SNe Ia. Having an independent set of distances will enable a deeper study of SN Ia systematic errors and evolution with redshift. A larger set of SN II light curves is also useful for efforts to better photometrically identify SN types. By having a more complete picture of the range and frequency of SN II light curve properties, positive identification of SNe II will be more likely, which will be useful both for building up a sample of SNe II and in excluding them with confidence from samples of other types, particularly SNe Ia. This will become increasingly important as large surveys provide far more SN light curves than spectroscopic identification resources can handle.

We thank the FLWO staff for their dedicated work in maintaining the 1.2 m and 1.5 m telescopes and instruments, as well as the 1.3 m PAIRITEL when it was in full operation. We likewise thank the MMT staff. We are grateful to Dan Scolnic for discussions on comparing the CfA SN II star sequences with the Pan-STARRS1 stars, and Carlos Contreras and Joseph Anderson for help comparing CfA SN II star sequences with the CSP. We also thank Kaisey Mandel and Arturo Avelino for helpful discussions. This work has been supported, in part, by NSF grants AST-0606772, AST-0907903, AST-1211196, and AST-1516854, and NASA grant NNX15AJ55G to Harvard University. A.S.F. acknowledges support from NSF Awards SES 1056580 and PHY 1541160. M. Modjaz is supported in part by the NSF CAREER award AST-1352405 and by the NSF award AST-1413260.

Facilities: FLWO:1.2m, FLWO: PAIRITEL, FLWO:1.5m, MMT.

ORCID iDs

Andrew S. Friedman  <https://orcid.org/0000-0003-1334-039X>
 Stephane Blondin  <https://orcid.org/0000-0002-9388-2932>
 Mike Calkins  <https://orcid.org/0000-0002-2830-5661>
 Thomas Matheson  <https://orcid.org/0000-0001-6685-0479>
 Maryam Modjaz  <https://orcid.org/0000-0001-7132-0333>

References

- Anderson, J. P., González-Gaitán, S., Hamuy, M., et al. 2014, *ApJ*, 786, 67
 Arcavi, I., Gal-Yam, A., Cenko, S. B., et al. 2012, *ApJL*, 756, L30
 Bianco, F. B., Modjaz, M., Hicken, M., et al. 2014, *ApJS*, 213, 19
 Blondin, S., Matheson, T., Kirshner, R. P., et al. 2012, *AJ*, 143, 126
 Bloom, J. S., Starr, D. L., Blake, C. H., Skrutskie, M. F., & Falco, E. E. 2006, in ASP Conf. Ser. 351, *Astronomical Data Analysis Software and Systems XV*, ed. D. P. C. Gabriel, C. Arviset, & E. Solano (San Francisco, CA: ASP), 751
 Cutri, R. M., Skrutskie, M. F., van Dyk, S., et al. 2003, The IRSA 2MASS All-Sky Point Source Catalog, NASA/IPAC Infrared Science Archive
 D'Andrea, C. B., Sako, M., Dilday, B., et al. 2010, *ApJ*, 708, 661
 de Jaeger, T., González-Gaitán, S., Hamuy, M., et al. 2017, *ApJ*, 835, 166
 Dessart, L., Blondin, S., Brown, P. J., et al. 2008, *ApJ*, 675, 644
 Eastman, R. G., Schmidt, B. P., & Kirshner, R. P. 1996, *ApJ*, 466, 911
 Fabricant, D. E., Cheimets, P., Caldwell, N., & Geary, J. 1998, *PASP*, 110, 79
 Faran, T., Poznanski, D., Filippenko, A. V., et al. 2014, *MNRAS*, 442, 844
 Fransson, C., Ergon, M., Challis, P., et al. 2014, *ApJ*, 797, 118
 Friedman, A. S. 2012, PhD thesis, Harvard Univ.
 Friedman, A. S., Wood-Vasey, W. M., Marion, G. H., et al. 2015, *ApJS*, 220, 9
 Galbany, L., González-Gaitán, S., Phillips, M. M., et al. 2016, *AJ*, 151, 33
 Gall, E. E. E., Kotak, R., Leibundgut, B., et al. 2017, arXiv:1705.10806
 Gall, E. E. E., Polshaw, J., Kotak, R., et al. 2015, *A&A*, 582, A3
 Gal-Yam, A. 2016, arXiv:1611.09353
 González-Gaitán, S., Tominaga, N., Molina, J., et al. 2015, *MNRAS*, 451, 2212
 Gutiérrez, C. 2016, Doctoral thesis, Universidad de Chile
 Hamuy, M., & Pinto, P. A. 2002, *ApJL*, 566, L63
 Hicken, M., Challis, P., Kirshner, R. P., et al. 2012, *ApJS*, 200, 12
 Hicken, M., Wood-Vasey, W. M., Blondin, S., et al. 2009, *ApJ*, 700, 331
 Jha, S., Kirshner, R. P., Challis, P., et al. 2006, *AJ*, 131, 527
 Kirshner, R. P., & Kwan, J. 1974, *ApJ*, 193, 27
 Kirshner, R. P., & Kwan, J. 1975, *ApJ*, 197, 415
 Liu, Y. Q., Modjaz, M., Bianco, F. B., & Graur, O. 2016, *ApJ*, 827, 90
 Maguire, K., Kotak, R., Smartt, S. J., et al. 2010, *MNRAS*, 403, L11
 Marion, G. H., Vinko, J., Kirshner, R. P., et al. 2014, *ApJ*, 781, 69
 Matheson, T., Blondin, S., Foley, R. J., et al. 2005, *AJ*, 129, 2352
 Matheson, T., Kirshner, R. P., Challis, P., et al. 2008, *AJ*, 135, 1598
 Modjaz, M., Blondin, S., Kirshner, R. P., et al. 2014, *AJ*, 147, 99
 Modjaz, M., Liu, Y. Q., Bianco, F. B., & Graur, O. 2016, *ApJ*, 832, 108
 Morozova, V., Piro, A. L., & Valenti, S. 2017, *ApJ*, 838, 28
 Pastorello, A., Benetti, S., Brown, P. J., et al. 2015, *MNRAS*, 449, 1921
 Planck Collaboration, Ade, P. A. R., Aghanim, M., et al. 2016, *A&A*, 594, A13
 Poznanski, D., Butler, N., Filippenko, A. V., et al. 2009, *ApJ*, 694, 1067
 Richardson, D., Branch, D., Casebeer, D., et al. 2002, *AJ*, 123, 745
 Riess, A. G., Kirshner, R. P., Schmidt, B. B., et al. 1999, *AJ*, 117, 707
 Riess, A. G., Macri, L. M., Hoffman, S. L., et al. 2016, *ApJ*, 826, 56
 Rodríguez, O., Clocchiatti, A., & Hamuy, M. 2014, *AJ*, 148, 107
 Rodríguez, O., Pignata, G., & Hamuy, M. 2016, http://sn2016.cl/documents/posters/poster_rodriguez.pdf
 Rubin, A., Gal-Yam, A., De Cia, A., et al. 2016, *ApJ*, 820, 33
 Sanders, N. E., Soderberg, A. M., Gezari, S., et al. 2015, *ApJ*, 799, 208
 Schechter, P. L., Mateo, M., & Saha, A. 1993, *PASP*, 105, 1342
 Schmidt, B. P., Kirshner, R. P., & Eastman, R. G. 1992, *ApJ*, 395, 366
 Schmidt, B. P., Kirshner, R. P., Eastman, R. G., et al. 1994, *ApJ*, 432, 42
 Scolnic, D., Casertano, S., Riess, A., et al. 2015, *ApJ*, 815, 117
 Skrutskie, M. F., Cutri, R. M., Stiening, R., et al. 2006, *AJ*, 131, 1163
 Smartt, S. J., Eldridge, J. J., Crockett, R. M., & Maund, J. R. 2009, *MNRAS*, 395, 1409
 Smith, J. A., Tucker, D. L., Kent, S., et al. 2002, *AJ*, 123, 2121
 Stritzinger, M. D., Phillips, M. M., Boldt, L. N., et al. 2011, *AJ*, 142, 156
 Taddia, F., Stritzinger, M. D., Sollerman, J., et al. 2013, *A&A*, 555, A10
 Tonry, J. L., Stubbs, C. W., Lykke, K. R., et al. 2012, *ApJ*, 750, 99
 Valenti, S., Howell, D. A., Stritzinger, M. D., et al. 2016, *MNRAS*, 459, 3939
 Van Dyk, S. D., Cenko, S. B., Poznanski, D., et al. 2012, *ApJ*, 756, 131
 Wood-Vasey, W. M., Friedman, A. S., Bloom, J. S., et al. 2008, *ApJ*, 689, 377